Supporting Information

Facile synthesis of Cu_2O microstructures and their morphology dependent electrochemical supercapacitor properties

Rudra Kumar, Prabhakar Rai,* Ashutosh Sharma*

Department of Chemical Engineering, Indian Institute of Technology Kanpur,

Kanpur 208016, India

*Corresponding authors; Email: prkrai@iitk.ac.in, ashutos@iitk.ac.in

Calculation of the Specific Capacitance;

(a) By using galvanostatic charge discharge method

$C= (I\times\Delta t)/ (m\times\Delta v) = (1\times10\text{-}3 \times264)/ (1\times10\text{-}3\times 0.4) =660$ F/g

(b) By cyclic voltammetry

$Cm=(1/m\times R\times\Delta V)\times \int I(v)dV = (1/1\times10\text{-}3\times2\times10\text{-}3\times0.7)\times 0.000903 = 645$ F/g

Figure S1 EDS spectra of the Cu_2O (a) microcubes and (b) microspheres.

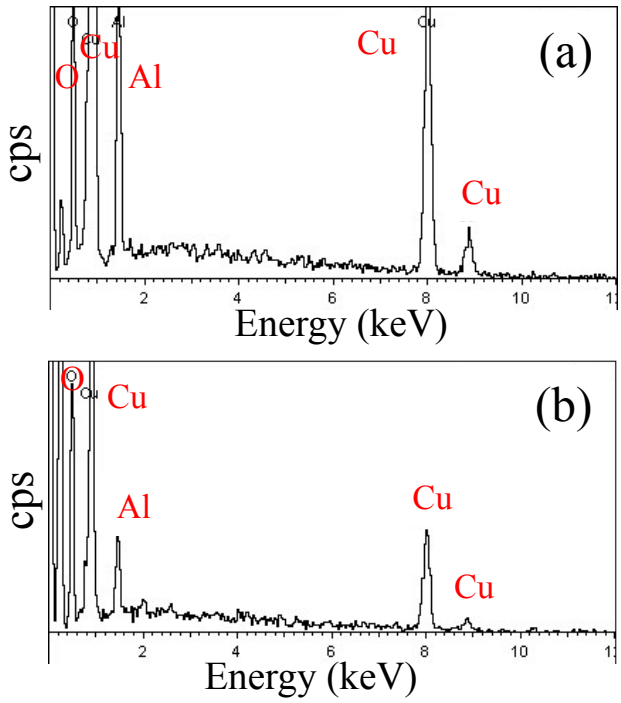

Figure S2 Nitrogen adsorption and desorption isotherms and corresponding pore size distribution curves (insets) of Cu_2O (a) microcubes and (b) microspheres.

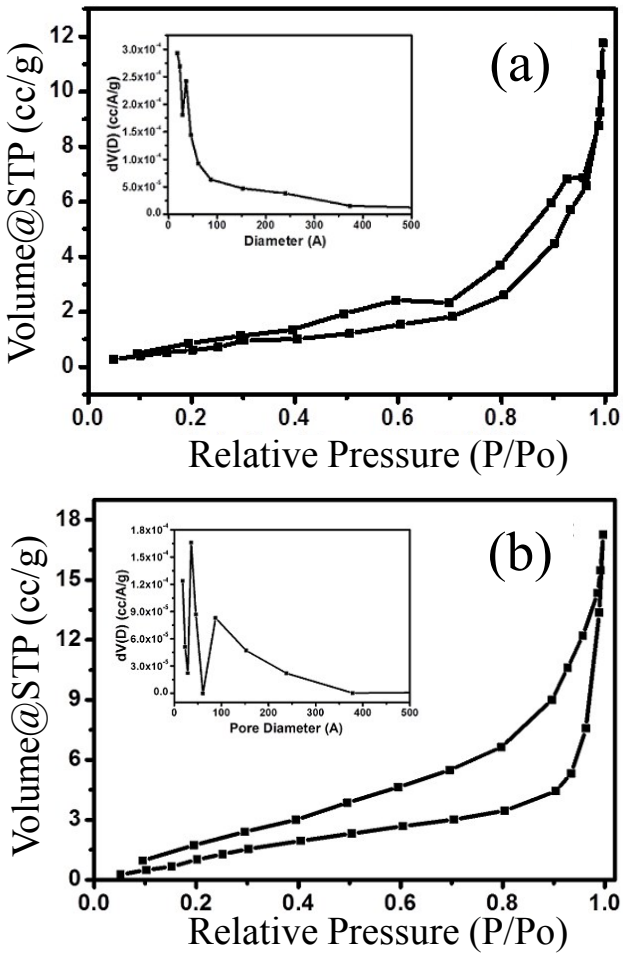

Figure S3 Specific capacitance of Cu_2O microcubes and microspheres at different scan rate.

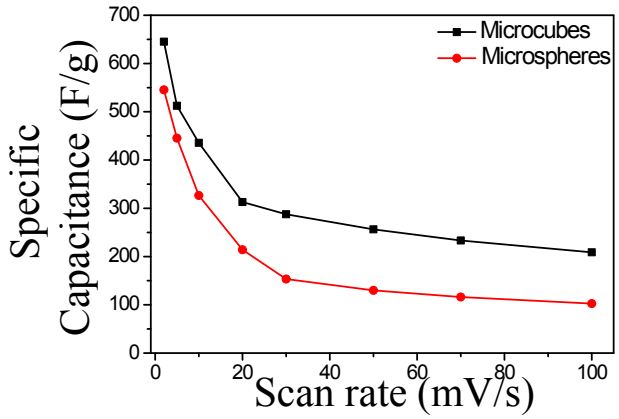

Figure S4 Cycling behaviour of Cu_2O microcubes at 5 and 10 A/g current density.

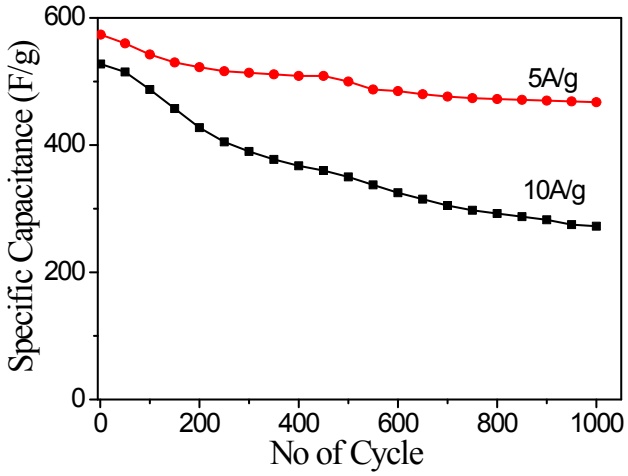

Figure S5 (a) CV curve at different electrolyte concentration at 50 mV/s scan rate, (b) cycling stability up to 500 cycle at 50 mV/s scan rate in 6M KOH, (c) Charge-discharge behaviour at different electrolyte concentration at 1A/g current density and (d) specific capacitance at different KOH concentration at 1A/g current density for Cu_2O microcubes.

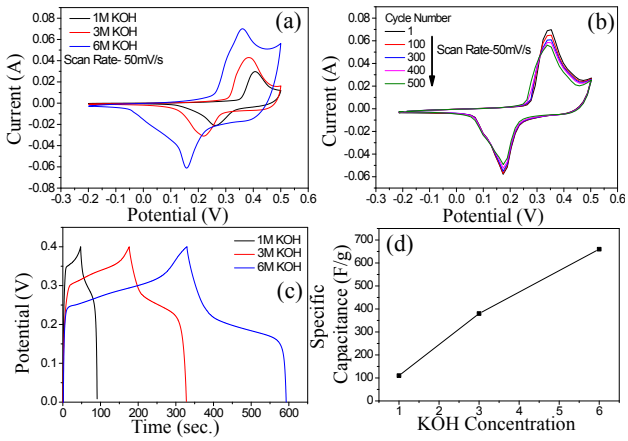

Figure S6 Coulombic efficiency of Cu_2O microcubes.

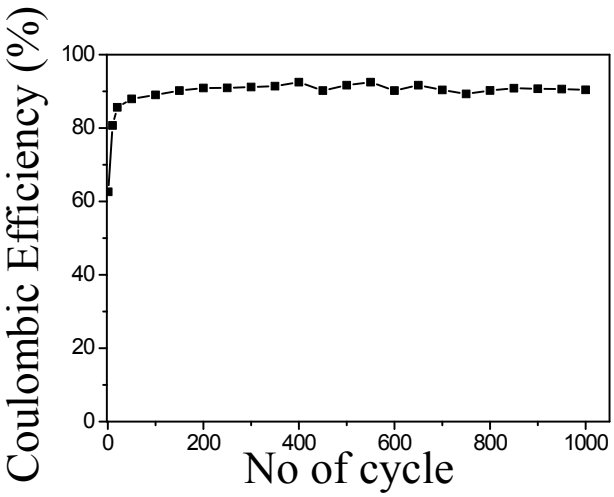

Figure S7 Nyquist plots of Cu_2O microcubes and microspheres.

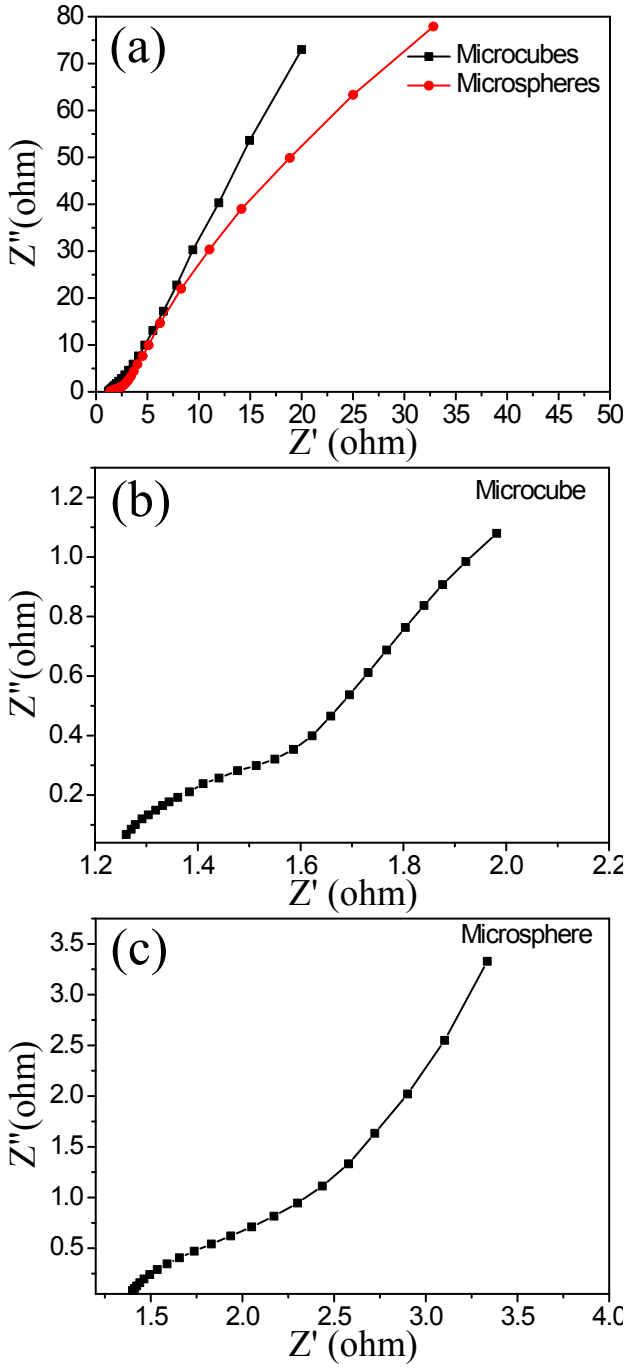

Figure S8 I-V curve measurement of Cu_2O microcubes and microspheres.

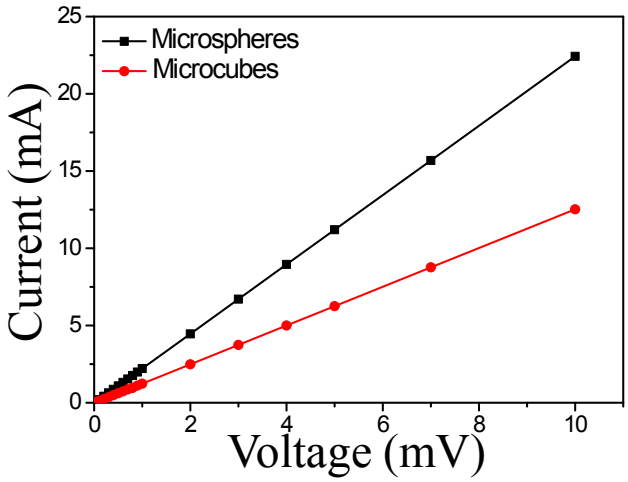

Table 1 Comparison of supercapacitor properties of Cu_2O microcubes with similar system reported in literature.

S. N.	Materials	Synthesis route	Specific Capacitance (F/g)	Capacitance Retention	Reference
1.	RGO–Cu_2O–TiO_2 ternary Nanocomposite,	Hydrothermal	80 F/g@ 0.2 A/g in 6 M KOH electrolyte, 41.4 F/g, 32.7 F/g	increases from 80 to 91.5 F/g after 1000 cycles	1
2.	RGO/Cu_2O composite films on Cu foil	Hydrothermal	98.5 F/g @1 A/g	50% after 1000 cycles	2
3	Cu@Cu_2O/graphene nanocomposites	Solvothermal	100.9 F/g at 0.1 A/g, 33.4 F/g	Capacitance increases from 100 F/g to 257 F/g after 1000 cycle	3
4	Cu_2O/RGO/Ni(OH)$_2$Nanocomposite	Hydrothermal	923.1 F/g @7.0 A/g	92.4% retention even after 4,000 cycles	4
5	Cu_2O@Reduced graphene oxide composite	Hydrothermal	31.0, 26.0, and 24.0 F/g @ 100, 200, and 400 mA/g	100 % retention even after 5,000 cycles	5
6	Three-dimensionally ordered macroporous Cu_2O/Ni inverse opal electrodes	Electrodeposition and Template method combined	502 F/g for 3DOM Cu_2O/Ni and 191 F/g Cu_2O/ flat Ni electrode	85% capacitance retention after 500 cycle at 10 mV/s	6
7	Cu_2O/CuO/RGO nanocomposite	Hydrothermal	173.4 F/g @ 1 A/g to 136.3 F/g @ 10 A/g	98.2% retention after 100,000 cycles at 10 A/g	7
8	3D binder-free Cu_2O@Cu nanoneedle arrays	Anodization of Cu foam and subsequent electro-oxidation	862.4 F/g @ 1 A/g	92% after retention after 10 000 cycles	8

9	mesoporous carbon electrodes with copper oxide nanoparticles	Silica template based	380 F/g @ 1mA/cm^2 with 20 wt % copper loading	96% retention after 5000 cycles @ 3mA/cm^2	9
10	CuO nanowires	Electrospinning	620 F/g @ 2 A/g,710 F/g @ 2mV/s	100 % retention after 2000 cycles	10
11	CuO nanosheet arrays grown on nickel foam	Template-free growth method	569 F/g @ a current density of 5mA/cm^2	82.5% retention after 500 cycles	11
12	Graphene-Like Copper Oxide Nanofilms	Anodisation process	919 F/g @ 1 A/g and 748 F/g @ 30 A/g	93% retention after 5000 cycles	12
13	CuO nanosheet clusters	Hydrothermal	535 F/g @5 mV/s	90% retention after 1000 cycles	13
14	Cu_2O Microcubes	Hydrothermal	660 F/g @ 1 A/g	80% retention after 1000 cycle @ 5 A/g	This work

References;

1. D. Luo, Y. Li, J. Liu, H. Feng, D. Qian, S. Peng, J. Jiang and Y. Liu, *J. Alloys Comp.*, 2013, **581**, 303–307.

2. X. Dong, K. Wang, C. Zhao, X. Qian, S. Chen, Z. Li, H. Liu and S. Dou, *J. Alloys Comp.*, 2014, **586**, 745–753.

3. Y. Li, Q. Wang, P. Liu, X. Yang, G. Dun and Y. Liu, *Ceramics International*, 2015, **41**, 4248–4253.

4. K. Wang, C. Zhao, S. Min and X. Qian, *Electrochimica Acta*, 2015, **165**, 314–322.

5. B. Li, H. Cao, G. Yin, Y. Lu and J. Yin, *J. Mater. Chem.*, 2011, **21**, 10645–10648.

6. M.-J. Deng, C.-Z. Song, P.-J. Ho, C.-C. Wang, J.-M. Chen and K.-T. Lu, *Phys. Chem. Chem. Phys.*, 2013, **15**, 7479—7483.

7. K. Wang, X. Dong, C. Zhao, X. Qian and Y. Xu, *Electrochimica Acta*, 2015, **152**, 433–442.

8. C. Dong, Y. Wang, J. Xu, G. Cheng, W. Yang, T. Kou, Z. Zhang and Y. Ding, *J. Mater. Chem. A*, 2014, **2**, 18229–18235.

9. K. P. S. Prasad, D. S. Dhawale, S. Joseph, C. Anand, M. A. Wahab, A. Mano, C.I. Sathish, V. V. Balasubramanian, T. Sivakumar and A. Vinu, *Microporous Mesoporous Materials*, 2013, **172**, 77–86.

10. B. Vidyadharan, I. I. Misnon, J. Ismail, M. M. Yusoff and R. Jose, *J. Alloys Comp.*, 2015, **633**, 22–30.

11. G. Wang, J. Huang, S. Chen, Y. Gao and D. Cao, *J. Power Sources*, 2011, **196**, 5756–5760.

12. Y. Lu, X. Liu,K. Qiu, J. Cheng, W. Wang, H. Yan, C. Tang, J.-K. Kim and Y. Luo, *ACS Appl. Mater. Interfaces*, 2015, **7**, 9682−9690.

13. G. S. Gund, D. P. Dubal, D. S. Dhawale, S. S. Shindea and C. D. Lokhande, *RSC Adv.*, 2013, **3**, 24099–24107.